

# Nonlinearity as Rank: Generative Low-Rank Adapters with Radial Basis Functions

Yihao Ouyang <sup>\*1</sup> Shiwei Li <sup>\*1</sup> Haozhao Wang <sup>1</sup> Xiandi Luo <sup>1</sup> Zhuoqi Hu <sup>1</sup> Yuetong Song <sup>2</sup> Qiyu Qin <sup>1</sup>  
Yichen Li <sup>1</sup> Ruixuan Li <sup>1</sup>

## Abstract

Low-rank adaptation (LoRA) approximates the update of a pretrained weight matrix using the product of two low-rank matrices. However, standard LoRA follows an **explicit-rank** paradigm, where increasing model capacity requires adding more rows or columns (i.e., **basis vectors**) to the low-rank matrices, leading to substantial parameter growth. In this paper, we find that these basis vectors exhibit significant parameter redundancy and can be compactly represented by lightweight nonlinear functions. Therefore, we propose **Generative Low-Rank Adapter (GenLoRA)**, which replaces explicit basis vector storage with nonlinear basis vector generation. Specifically, GenLoRA maintains a latent vector for each low-rank matrix and employs a set of lightweight radial basis functions (RBFs) to synthesize the basis vectors. Each RBF requires far fewer parameters than an explicit basis vector, enabling higher parameter efficiency in GenLoRA. Extensive experiments across multiple datasets and architectures show that GenLoRA attains higher effective LoRA ranks under smaller parameter budgets, resulting in superior fine-tuning performance. The code is available at <https://anonymous.4open.science/r/GenLoRA-1519>.

## 1. Introduction

Large language models (LLMs) have demonstrated unprecedented capabilities across a wide range of tasks (Dubey et al., 2024; DeepSeek et al., 2024; Cai et al., 2024). To adapt these general-purpose models to specific downstream applications, fine-tuning is essential. However, as model sizes explode, full fine-tuning becomes prohibitive in both computa-

<sup>\*</sup>Equal contribution <sup>1</sup>Huazhong University of Science and Technology, Wuhan, China <sup>2</sup>Hebei University of Technology, Tianjin, China. Correspondence to: Ruixuan Li <rxli@hust.edu.cn>.

Preprint. February 6, 2026.

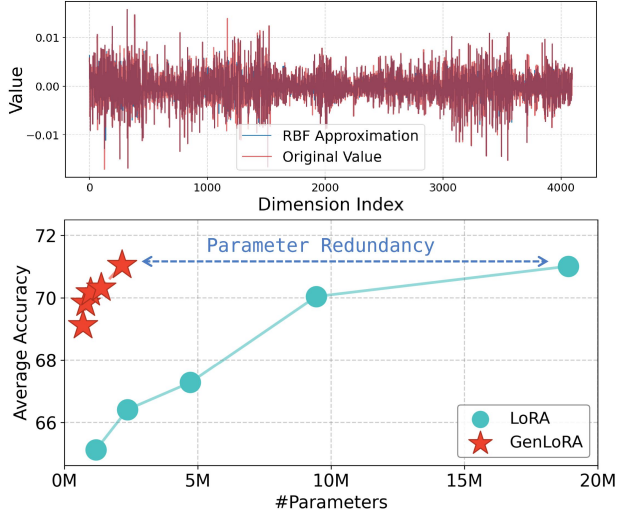


*Figure 1. (Upper)* The reconstruction result of the first row vector of a pretrained LoRA matrix  $B$ . The trajectories in **hue** illustrate the overlap between the Radial Basis Function (RBF) approximation and the original values. *(Lower)* Accuracy–parameter trade-off on mathematical reasoning tasks with LLaMA3-8B. The five points for each method correspond to ranks  $r = \{2, 4, 8, 16, 32\}$ .

tation and memory. Parameter-efficient fine-tuning (PEFT) methods (Lester et al., 2021; Houldsby et al., 2019) have thus emerged as a standard paradigm, among which low-rank adaptation (LoRA) (Hu et al., 2022) is widely adopted. LoRA approximates the update of a pretrained weight  $W \in \mathbb{R}^{m \times n}$  as a low-rank decomposition  $\Delta W = BA$ , where  $B \in \mathbb{R}^{m \times r}$  and  $A \in \mathbb{R}^{r \times n}$ , with  $r \ll \min(m, n)$ .

The effectiveness of LoRA is closely tied to the rank  $r$ , as a larger rank generally increases the expressive capacity of the adaptation. However, LoRA follows an explicit-rank paradigm: increasing  $r$  requires maintaining additional independent basis vectors, corresponding to the columns of  $B$  and the rows of  $A$ . In modern LLMs, the projection dimensions  $m$  and  $n$  are typically on the order of thousands, which makes this expansion costly. Specifically, as the rank increases, the total number of parameters grows linearly with  $m + n$ , leading to a parameter complexity of  $\mathcal{O}(r(m + n))$ . This scaling behavior motivates a natural question: *do these*

**high-dimensional basis vectors contain parameter redundancy that can be exploited for more efficient adaptation?**

To examine the suspected parameter redundancy, we study learnable non-linear functions for basis vector reconstruction. Specifically, given a pretrained LoRA matrix containing  $r$  basis vectors, we first construct a shared prototype vector by averaging these  $r$  basis vectors. We then learn  $r$  independent non-linear functions that take this shared prototype as input and reconstruct the original  $r$  basis vectors. In this work, we focus on Radial Basis Functions (RBFs) (Buhmann, 2000), which are renowned for their powerful approximation capabilities and high parameter efficiency. Additional details of the experimental setup are provided in the Appendix I.3. As shown in Figure 1 (*Upper*), the results are compelling: the RBFs successfully recover the global shape and essential patterns of the original basis vectors. Most strikingly, this reconstruction requires very few learnable parameters, amounting to only 6.25% of the parameters needed to define a single basis vector. This finding affirmatively answers our research question: substantial parameter redundancy indeed exists within the explicit basis vectors, as the information spread across them can be effectively compressed into non-linear transformations. In essence, nonlinearity can serve as a parameter-efficient substitute for rank, offering a direct solution to the identified redundancy, which we term “Nonlinearity as Rank”.

To address the parameter redundancy described above, we propose **Generative Low-Rank Adapters** (GenLoRA), which generate basis vectors through nonlinearity rather than storing them as explicit parameters. Specifically, GenLoRA maintains a single learnable latent vector for each low-rank matrix ( $A$  or  $B$ ) and learns  $r$  RBF-based non-linear generators. Each generator maps the shared latent vector to one basis vector, and the resulting  $r$  generated vectors directly form the matrices  $A$  and  $B$ . This design allows the effective rank to scale while keeping the parameter complexity at  $\mathcal{O}(m + n + r|\theta|)$ , where  $|\theta|$  denotes the number of parameters in each generator and typically satisfies  $|\theta| \ll \min(m, n)$ . As illustrated in Figure 1 (*Lower*), this formulation effectively removes the substantial parameter redundancy in standard LoRA and yields a better accuracy–parameter trade-off. In addition, theoretical analysis shows that GenLoRA preserves the low-rank structure and guarantees bounded gradients, enabling stable training.

Our main contributions are summarized as follows:

- We reveal significant parameter redundancy in LoRA through the basis vector reconstruction experiment. The results show that basis vectors can be effectively represented by non-linear functions, establishing nonlinearity as a parameter-efficient substitute for rank.
- We propose GenLoRA, the first generative LoRA

framework that synthesizes lora-rank matrices from shared latent vectors via RBF generators. This design mitigates the parameter redundancy, allowing effective rank increase with only minimal parameter cost.

- We conduct extensive experiments on multiple models and datasets, demonstrating that GenLoRA consistently outperforms LoRA and its variants. Specifically, GenLoRA achieves 2-4% improvement on natural language generation tasks and 6-8% on code generation, while utilizing fewer trainable parameters.

## 2. Related Work

### 2.1. Low-Rank Adaptation

To reduce fine-tuning overhead, LoRA (Hu et al., 2022) approximates weight updates  $\Delta W$  via two low-rank matrices  $B$  and  $A$ . Recent studies have refined this paradigm, primarily focusing on three directions: optimization, linear structural adjustments, and nonlinear extensions. Optimization-centric methods enhance stability and initialization; for instance, DoRA (Liu et al., 2024a) decouples magnitude and direction updates, LoRA+ (Hayou et al., 2024) employs differential learning rates, while PiSSA (Meng et al., 2024) and LoRA-GA (Wang et al., 2024) leverage SVD for better initialization. To mitigate the low-rank bottleneck, linear variants manipulate rank structure: AdaLoRA (Zhang et al., 2023) and TopLoRA (Li et al., 2025b) utilize dynamic rank allocation or token-wise projections, while HiRA (Huang et al., 2025), KronA (Edalati et al., 2025), and MELORA (Ren et al., 2024) employ Hadamard products, Kronecker products, or diagonal stacking to approximate higher-rank updates. Alternatively, NOLA (Koohpayegani et al., 2023) and HyperLoRA (Li et al., 2025a) reconstruct weights via linear combinations of random or learned basis matrices. Recognizing the limits of linearity, nonlinear variants like LoRAN (Li et al., 2024), SineLoRA (Ji et al., 2024), and AuroRA (Dong et al., 2025) introduce nonlinearity. AuroRA restricts nonlinearity to the **low-dimensional activation space**; however, it is often insufficient to capture complex dependencies due to the persistent information bottleneck. Instead, GenLoRA operates in a **high-dimensional parameter generation space**. By utilizing nonlinearity to generate high-dimensional information, GenLoRA bypasses this bottleneck, achieving superior expressiveness with minimal marginal parameter cost. Furthermore, unlike NOLA and HyperLoRA which generate mixing coefficients for shared bases, our method directly generates the basis matrices themselves.

### 2.2. Nonlinearity Applications

The pursuit of expressive approximation has long driven the evolution of nonlinear basis functions, ranging from

rational functions (Baker Jr, 1963) and trigonometric functions (Edmunds et al., 2012) to locally supported basis functions like B-splines (De Boor, 1972) and Radial Basis Functions (RBFs) (Buhmann, 2000). Specific nonlinear forms have been instrumental in recent advancements. For instance, NoRA (Yin et al., 2025) applies rational functions to construct learnable activation functions with a numerator-denominator structure, demonstrating that optimizing the shape of activation functions is as substantial as optimizing weights. Similarly, trigonometric bases have been explored in works like SineLoRA (Ji et al., 2024) and FourierFT (Gao et al., 2024) to introduce periodic modulations or spectral transforms into low-rank updates.

More recently, the Kolmogorov-Arnold Network (KAN) (Liu et al., 2024b) represents a paradigm shift; based on the Kolmogorov-Arnold representation theorem, it shifts the learning focus from linear weights to parameterizable activation functions. Aurora (Dong et al., 2025) subsequently enhances adaptation flexibility by integrating KAN-based non-linear MLP layers. However, unlike methods that operate as **parameter-heavy MLP layers** which incur substantial overhead, GenLoRA minimizes parameter overhead by leveraging **learnable non-linear functions** strictly for weight generation. Furthermore, we strategically replace the computationally intensive B-splines typical of KANs with Radial Basis Functions (RBFs). This choice significantly boosts computational efficiency without compromising approximation accuracy, offering a robust and lightweight solution for high-dimensional parameter generation.

### 3. Methodology

In this section, we introduce **Generative Low-Rank Adapters (GenLoRA)**, a novel paradigm designed to synthesize high-dimensional basis vectors from a latent vector via lightweight Radial Basis Function (RBF) generators.

#### 3.1. Nonlinearity as Rank

We first revisit LoRA from a generative perspective. As illustrated in Figure 2(a), we characterize standard LoRA as adhering to an explicit-rank paradigm, where the low-rank structure is directly constructed from independent and trainable explicit basis vectors. Given a frozen weight matrix  $W_0 \in \mathbb{R}^{m \times n}$ , standard LoRA learns a low-rank update:

$$\Delta W = BA = \sum_{i=1}^r b_i a_i^\top, \quad (1)$$

where the matrices are composed of explicit basis vectors:  $B = [b_1, \dots, b_r] \in \mathbb{R}^{m \times r}$  and  $A = [a_1, \dots, a_r]^\top \in \mathbb{R}^{r \times n}$ . Here,  $b_i \in \mathbb{R}^m$  and  $a_i \in \mathbb{R}^n$  denote the  $i$ -th column of  $B$  and the  $i$ -th row of  $A$ , respectively. This implies that each incremental rank unit incurs a parameter cost of  $m + n$ , resulting in a total complexity of  $\mathcal{O}(r(m + n))$ .

We propose to treat nonlinearity as a substitute for explicit basis vectors: instead of introducing a massive number of parameters for storage, we synthesize these vectors using a minimal set of parameters as illustrated in Figure 2(b). Formally, GenLoRA reparameterizes matrices  $B$  and  $A$  via latent vectors and nonlinear generators. Let  $Z_B \in \mathbb{R}^{m \times 1}$  and  $Z_A \in \mathbb{R}^{1 \times n}$  be two learnable latent vectors. Let  $F_B = \{f_1^B, \dots, f_r^B\}$  and  $F_A = \{f_1^A, \dots, f_r^A\}$  be two sets of lightweight nonlinear generators. Each generator takes the corresponding latent vector  $Z_B$  or  $Z_A$  as input to synthesize a basis vector:

$$\begin{aligned} b_i &= f_i^B(Z_B; \theta_i^B) \in \mathbb{R}^m, \\ a_i &= f_i^A(Z_A; \theta_i^A) \in \mathbb{R}^n, \end{aligned} \quad (2)$$

where  $\theta_i^B$  and  $\theta_i^A$  are the parameters of the nonlinear generators, and we use  $\theta$  to denote the generator parameters when no distinction is required. Stacking these vectors reconstructs the low-rank matrices:

$$B = [b_1, \dots, b_r], \quad A = [a_1, \dots, a_r]^\top, \quad (3)$$

resulting in the GenLoRA update:

$$\Delta W_{\text{Gen}} = \sum_{i=1}^r f_i^B(Z_B; \theta_i^B) f_i^A(Z_A; \theta_i^A)^\top. \quad (4)$$

Under this parameterization, the number of trainable parameters is primarily determined by the sizes of  $Z_B$ ,  $Z_A$ , and the nonlinear generators. Specifically, the parameter complexity is  $\mathcal{O}(m + n + r|\theta|)$ , where  $|\theta|$  denotes the number of parameters for a pair of  $f_i^A$  and  $f_i^B$ . Since  $|\theta| \ll m, n$ , this complexity is substantially lower than the  $\mathcal{O}(r(m + n))$  parameter cost of standard LoRA. By exploiting the expressive power of nonlinear mappings from latent vectors to basis vectors, GenLoRA significantly enhances adapter capacity, thereby realizing our core principle of Nonlinearity as Rank.

#### 3.2. RBF-based Functional Generators

Radial basis functions (RBFs) are well known for their strong approximation capability and high parameter efficiency. Motivated by these properties, we instantiate the nonlinear generators  $f_i^B$  and  $f_i^A$  using RBF-based parameterizations. To further achieve stable and expressive non-linear mapping, we introduce instance-wise normalization and group-wise decomposition in the generator design, as shown in Figure 2(c).

**Group-wise decomposition.** Let  $z \in \mathbb{R}^d$  denote an input latent vector. To avoid directly high-dimensional mapping, we partition  $z$  into  $G$  low-dimensional sub-vectors  $\{\mathbf{x}_1, \dots, \mathbf{x}_G\}$ , where each  $\mathbf{x}_g \in \mathbb{R}^{d_g}$  such that  $d = G \cdot d_g$ . To ensure that the  $r$  synthesized basis vectors remain distinct and avoid rank collapse, each basis vector is generated using

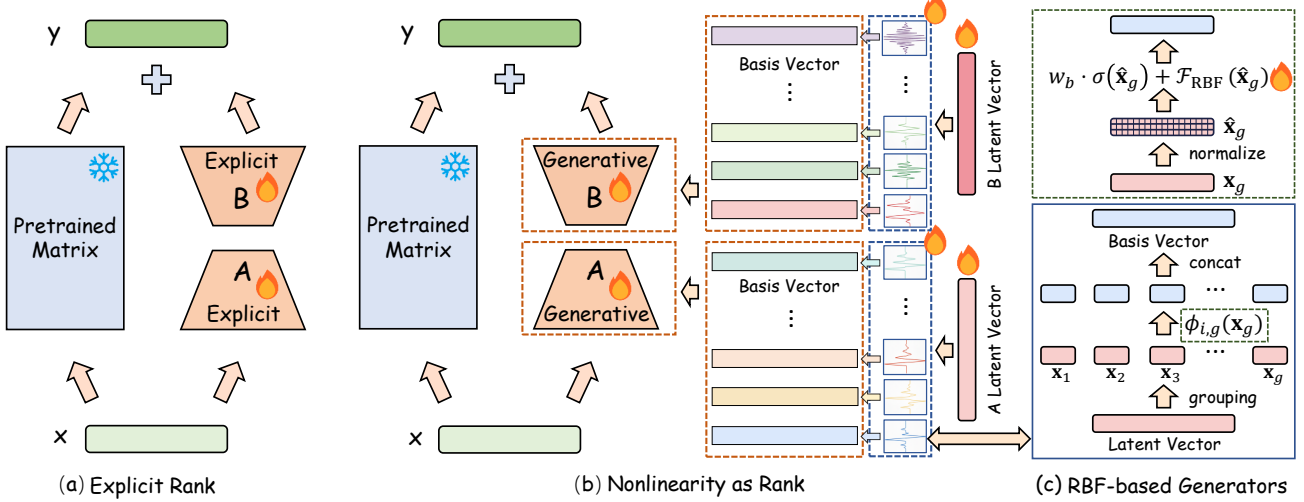


Figure 2. The overall architecture of Generative Low-Rank Adapters (GenLoRA). (a) **Explicit Rank**: Standard LoRA relies on the explicit-rank paradigm, where model capacity is constrained by the linear dimension of basis vectors. (b) **Nonlinearity as Rank**: Our proposed paradigm synthesizes basis vectors from latent vectors via generative functions, effectively reducing the parameter cost. (c) **RBF-based Generators**: The detailed internal workflow of the generator. High-dimensional latent vectors undergo group-wise decomposition and instance-wise normalization to ensure stability and effectiveness. The final basis vectors are synthesized by aggregating weighted Gaussian Radial Basis Functions combined with a linear residual term.

$r$  nonlinear generators, and each generator  $f_i$  processes its corresponding sub-vectors using  $g$  distinct transformations:

$$f_i(z) = \text{concat}(\phi_{i,1}(x_1), \dots, \phi_{i,G}(x_G)) \in \mathbb{R}^d, \quad (5)$$

where  $\phi_{i,g}$  represents the specific transformation corresponding to the  $g$ -th sub-vector within the  $i$ -th generator. This decomposition reduces the mapping dimensionality of the nonlinear functions, effectively mitigating mapping complexity while enhancing their expressiveness. Furthermore, the independence of these sub-mappings enables parallel processing, significantly reducing computational overhead.

**Instance-wise normalization.** The learned nonlinear generators are designed to operate on inputs within a predefined interval, known as the grid range. However, since the numerical distribution of the input latent vectors is typically unknown and dynamic, manually adapting the fixed RBF grid to cover all input values is impractical. This mismatch often causes some input features to fall outside the effective receptive field of the grid basis functions, reducing approximation efficiency. To resolve this, instead of adjusting the grid, we normalize the input features to match a standard distribution. For the  $g$ -th sub-vector  $x_g$ , we compute the normalized vector  $\hat{x}_g$ :

$$\hat{x}_g = \frac{x_g - \mu_g}{\sigma_g + \varepsilon}, \quad (6)$$

where  $\mu_g$  and  $\sigma_g$  are the mean and standard deviation of  $x_g$  and  $\varepsilon$  is for stability. By normalizing inputs, we can confidently set the fixed grid range to  $[-3, 3]$ . According to the

properties of the standard normal distribution, this interval covers approximately 99.7% of the data points, ensuring that input features are uniformly captured by the RBF grid and preventing fitting failures caused by distribution shifts.

Finally, the generator synthesizes values by combining a base linear transformation with an RBF nonlinear expansion. Using the normalized vector  $\hat{x}_g$  from Eq. 6, we define the transformation  $\phi_{i,g}$  applied to the sub-vector  $x_g$  as:

$$\phi_{i,g}(x_g) = w_b \cdot \sigma(\hat{x}_g) + \mathcal{F}_{\text{RBF}}(\hat{x}_g), \quad (7)$$

where  $\sigma(\cdot)$  is a standard activation function (e.g., SiLU),  $w_b$  is a learnable scalar scaling weight specific to this group, and  $\mathcal{F}_{\text{RBF}}(\cdot)$  represents the expressive RBF-based nonlinear term which will be detailed in Sec. 3.3.

### 3.3. Gaussian Radial Basis Functions

Given the normalized input distribution, we define a grid of  $K$  uniform centers  $\{\mu_k\}_{k=1}^K$  over a fixed interval. The element-wise response of the  $k$ -th Gaussian basis function to the normalized input sub-vector  $\hat{x}_g$  is:

$$\varphi_k(\hat{x}_g) = \exp\left(-\left(\frac{\hat{x}_g - \mu_k}{h}\right)^2\right), \quad (8)$$

where  $h$  is the bandwidth determined by the grid spacing, and the operations are applied element-wise.

The final nonlinear output is a linear combination of these basis responses. Let  $W_{\text{rbf}} = \{w_1, \dots, w_K\} \in \mathbb{R}^K$  denote the learnable weight vector associated with the current

group. The function  $\mathcal{F}_{\text{RBF}}(\hat{\mathbf{x}}_g)$  is defined as:

$$\mathcal{F}_{\text{RBF}}(\hat{\mathbf{x}}_g) = \sum_{k=1}^K w_k \cdot \varphi_k(\hat{\mathbf{x}}_g). \quad (9)$$

In implementation, Eqs. (8) and (9) are vectorized via broadcasting, leveraging GPU parallelism for efficient inference.

### 3.4. Theoretical Analysis

We now analyze the theoretical properties of GenLoRA, focusing on the algebraic structure of the weight updates and optimization stability. These analyses confirm that our “Nonlinearity as Rank” paradigm preserves low-rank constraints while ensuring robust training dynamics.

**Proposition 3.1** (Rank Boundedness). *Let  $\Delta W_{\text{Gen}} \in \mathbb{R}^{m \times n}$  be the weight update generated by GenLoRA with  $r$  pairs of generator functions  $\{f_i^B\}_{i=1}^r$  and  $\{f_i^A\}_{i=1}^r$ , where  $r \ll \min(m, n)$ . The rank of the update matrix satisfies:*

$$\text{rank}(\Delta W_{\text{Gen}}) \leq r. \quad (10)$$

Proposition 3.1 theoretically guarantees that GenLoRA does not violate the low-rank assumption. Although the mapping from latent space to weight space is highly nonlinear, the geometric structure of the final update remains strictly confined to an  $r$ -dimensional subspace. The corresponding proof is provided in Appendix A.

**Proposition 3.2** (Gradient Boundedness). *In GenLoRA, the gradients of the loss function  $\mathcal{L}$  with respect to the latent vectors  $Z_A, Z_B$  and generator weights  $\Theta_A, \Theta_B$  are locally bounded. That is, for any bounded parameter set, there exist constants  $C_1, C_2 > 0$  such that*

$$\left\| \frac{\partial \mathcal{L}}{\partial Z} \right\| < C_1, \quad \left\| \frac{\partial \mathcal{L}}{\partial \Theta} \right\| < C_2. \quad (11)$$

Proposition 3.2 arises from two key mechanisms in our design. First, the instance-wise normalization (Eq. (6)) ensures that the inputs to the RBF generators lie within a stable, numerically bounded range. Second, the Gaussian RBFs (Eq. (8)) and their derivatives are inherently bounded and smooth functions. This combination effectively prevents the risk of exploding gradients, ensuring that GenLoRA can be trained stably even with a high effective rank  $r$ . A detailed proof is provided in Appendix B.

## 4. Experiments

In this section, we evaluate GenLoRA on three benchmarks across various architectures, followed by ablation studies verifying its scalability and visualizing singular values.

### 4.1. Experimental Settings

**Models and Datasets.** First, we evaluate the natural language generation (NLG) capabilities of GenLoRA on the mathematical reasoning (Math10K) (Hu et al., 2023) and commonsense reasoning (Commonsense170K) benchmarks (Hu et al., 2023). Both benchmarks comprise a training corpus and multiple test sub-tasks. For each benchmark, we fine-tune the models on the training data and subsequently assess performance across all sub-tasks. To demonstrate the versatility of GenLoRA, we conduct experiments utilizing various model architectures and scales, including Gemma-7B (Team et al., 2024), LLaMA-3-8B (Dubey et al., 2024), and Qwen2.5-14B (Yang et al., 2024). Next, we assess the code generation capability of GenLoRA using LLaMA-3-8B (Dubey et al., 2024). We fine-tune the model on the Magicoder-Evol-Instruct-110k dataset (Wei et al., 2023), a curated and decontaminated subset of WizardCoder (Luo et al., 2023) comprising high-quality instruction-response pairs for programming tasks. Subsequently, we assess the performance on the Humaneval+ test with 50 sampled completions per problem. We report Pass@1, Pass@5, and Pass@10 accuracy following the standard protocol via the BigCode Evaluation Harness (Allal et al., 2022).

**Baseline Methods.** GenLoRA is compared with several baseline methods to demonstrate the effectiveness of our approach, including LoRA (Hu et al., 2022), along with prominent variants: DORA (Liu et al., 2024a), MELoRA (Ren et al., 2024), HiRA (Huang et al., 2025), and Aurora (Dong et al., 2025). These methods represent diverse approaches to improving LoRA: magnitude-direction decomposition, ensemble strategies, matrix product approximations, and nonlinear transformations. A comparison with these methods clearly highlights the superiority of GenLoRA. Details on the baselines are provided in Appendix I.2.

### 4.2. Overall Performance

**Results on Mathematical Reasoning Tasks.** As shown in Table 1, GenLoRA demonstrates robust scalability and superior performance across diverse model architectures, consistently achieving higher accuracy with significantly fewer parameters. Specifically, on LLaMA3-8B, GenLoRA ( $r = 8$ ) outperforms LoRA by an average of 2.3% while utilizing only about one-fifth of the parameters (0.98M vs. 4.72M). This advantage extends to 3.18% at rank 32, where the parameter count remains less than half of the baseline. Similarly, on Qwen2.5-14B and Gemma-7B, GenLoRA achieves the highest average accuracy, surpassing all rank-8 baselines while requiring merely a fraction of their parameter budget. In comparison, Aurora, which aims to optimize the trade-off between parameter efficiency and model expressivity, falls short against GenLoRA. For instance, on the LLaMA3 benchmark, GenLoRA ( $r = 8$ ) not only surpasses

Table 1. The accuracy on Mathematical Reasoning tasks (Math10K) with various pretrained models.

| Method      | #Params                                      | AddSub | MultiArith | SingleEq | SVAMP | gsm8k | AQuA  | Avg          |
|-------------|--|--------|------------|----------|-------|-------|-------|--------------|
| LLaMA-3-8B  | LoRA ( $r = 8$ )                             | 4.72M  | 82.28      | 85.83    | 89.76 | 66.40 | 56.18 | 23.23        |
|             | MELoRA ( $r = 8$ )                           | 4.72M  | 83.80      | 84.00    | 86.61 | 62.90 | 47.84 | 22.83        |
|             | HiRA ( $r = 8$ )                             | 4.72M  | 85.82      | 88.16    | 91.34 | 68.90 | 54.66 | 27.55        |
|             | DoRA ( $r = 8$ )                             | 4.92M  | 83.04      | 87.67    | 91.14 | 66.60 | 56.41 | 21.65        |
|             | Aurora ( $r = 2$ )                           | 1.18M  | 80.00      | 83.67    | 88.19 | 64.40 | 50.27 | 25.59        |
|             | Aurora ( $r = 8$ )                           | 4.72M  | 80.25      | 87.50    | 89.57 | 67.30 | 56.86 | 20.47        |
|             | <b>GenLoRA (<math>r = 8, g = 16</math>)</b>  | 0.98M  | 88.35      | 90.67    | 93.70 | 70.80 | 53.90 | 23.62        |
| Gemma-7B    | <b>GenLoRA (<math>r = 32, g = 16</math>)</b> | 2.16M  | 87.09      | 92.71    | 94.49 | 70.80 | 56.18 | 25.59        |
|             | LoRA ( $r = 8$ )                             | 4.82M  | 86.58      | 89.33    | 89.57 | 72.70 | 56.71 | 30.71        |
|             | MELoRA ( $r = 8$ )                           | 4.82M  | 84.81      | 89.00    | 89.96 | 71.40 | 55.12 | 29.53        |
|             | HiRA ( $r = 8$ )                             | 4.82M  | 85.85      | 88.67    | 90.55 | 72.10 | 55.04 | 26.38        |
|             | DoRA ( $r = 8$ )                             | 5.16M  | 86.58      | 90.33    | 90.16 | 76.00 | 57.09 | 26.38        |
|             | Aurora ( $r = 2$ )                           | 1.20M  | 85.82      | 87.33    | 88.58 | 73.60 | 56.86 | 27.95        |
|             | <b>GenLoRA (<math>r = 8, g = 16</math>)</b>  | 0.95M  | 84.56      | 91.33    | 90.94 | 71.00 | 56.86 | 28.74        |
| Qwen2.5-14B | <b>GenLoRA (<math>r = 16, g = 16</math>)</b> | 1.29M  | 87.34      | 92.17    | 90.55 | 71.80 | 56.19 | 28.35        |
|             | LoRA ( $r = 8$ )                             | 8.65M  | 91.14      | 96.17    | 92.52 | 86.10 | 75.51 | 33.46        |
|             | MELoRA ( $r = 8$ )                           | 8.65M  | 92.91      | 94.00    | 91.73 | 83.60 | 74.75 | 31.89        |
|             | HiRA ( $r = 8$ )                             | 8.65M  | 92.41      | 94.67    | 91.14 | 84.40 | 75.21 | 35.43        |
|             | DoRA ( $r = 8$ )                             | 8.99M  | 93.16      | 96.00    | 92.52 | 85.50 | 75.28 | 33.86        |
|             | Aurora ( $r = 2$ )                           | 2.16M  | 93.41      | 95.00    | 91.73 | 84.10 | 73.24 | 33.07        |
|             | <b>GenLoRA (<math>r = 8, g = 8</math>)</b>   | 1.38M  | 92.15      | 96.00    | 92.13 | 85.90 | 76.19 | 35.83        |
|             | <b>GenLoRA (<math>r = 32, g = 8</math>)</b>  | 2.26M  | 91.65      | 96.17    | 93.31 | 87.80 | 74.68 | 38.58        |
|             |  |        |            |          |       |       |       | <b>80.36</b> |

Aurora ( $r = 8$ ) by over 3% in accuracy but does so using approximately 80% fewer parameters. This clearly demonstrates that GenLoRA provides a far superior solution to the efficiency-performance trade-off.

**Results on Commonsense Reasoning Tasks.** As shown in Table 2, GenLoRA also achieves the best accuracy in commonsense reasoning tasks. The experimental conclusions are highly consistent with those in mathematical reasoning tasks. At the same rank ( $r = 8$ ), GenLoRA’s accuracy across the three models is, on average, 1.4% higher than that of LoRA, while requiring more than four times fewer parameters (0.98M vs. 4.72M). Furthermore, increasing the rank allows GenLoRA to further extend these gains, delivering absolute improvements of up to 2.7% on LLaMA3-8B and Gemma-7B compared to the standard LoRA baseline. Notably, even with this expanded capacity, GenLoRA still utilizes less than half the parameter budget of the rank-8 baselines, demonstrating extreme parameter efficiency.

**Results on Code Generation Tasks.** As presented in Table 3, GenLoRA consistently outperforms competing methods on the code generation task using the LLaMA3-8B model. Specifically, GenLoRA ( $r = 8$ ) delivers comprehensive improvements across Pass@1, Pass@5, and Pass@10 metrics compared to standard LoRA, while utilizing merely about one-fifth of the parameters. Scaling GenLoRA to

a rank of 32 yields further substantial gains; compared to standard LoRA, GenLoRA ( $r = 32$ ) achieves absolute improvements of +7.51% in Pass@1, +6.44% in Pass@5, and +6.46% in Pass@10, demonstrating significant performance margins over other competitive baselines. Notably, even with the expanded capacity at rank 32, GenLoRA (2.16M) operates with less than half the parameter count of the standard rank-8 baselines, highlighting its parameter efficiency.

**Efficiency Analysis.** Beyond performance gains, we assess the computational overhead in Table 3. Remarkably, GenLoRA ( $r = 8$ ) achieves a training time of 11.7h, corresponding to a relative time of 1.01 $\times$ , comparable to the efficiency of standard LoRA. We attribute this low latency primarily to the utilization of Radial Basis Functions. Unlike B-spline functions, which suffer from exponential complexity scaling on high-dimensional data, the core RBF computation relies on pure tensor operations such as vectorized element-wise exponentiations and matrix multiplications. This structure is inherently suited for massive GPU parallelism, enabling GenLoRA to introduce powerful expressive capabilities with minimal computational overhead.

### 4.3. Ablation Studies

Next, we conduct ablation studies on the LLaMA3-8B model to validate the effectiveness of our proposed Instanc-

Table 2. The accuracy on Commonsense Reasoning benchmarks with various pretrained models.

| Method      | #Params                             | OBQA  | ARC-C | Wino  | PIQA  | Social | ARC-E | BoolQ | Hella | Avg   |              |
|-------------|-------------------------------------|-------|-------|-------|-------|--------|-------|-------|-------|-------|--------------|
| LLaMA-3-8B  | LoRA ( $r = 8$ )                    | 4.72M | 81.60 | 78.50 | 82.08 | 87.54  | 77.79 | 91.67 | 70.40 | 87.95 | 82.19        |
|             | MELoRA ( $r = 8$ )                  | 4.72M | 74.80 | 75.00 | 71.43 | 84.71  | 72.98 | 89.44 | 67.74 | 80.84 | 77.12        |
|             | HiRA ( $r = 8$ )                    | 4.72M | 84.40 | 80.29 | 85.40 | 89.01  | 79.43 | 91.96 | 65.44 | 92.17 | 83.51        |
|             | DoRA ( $r = 8$ )                    | 4.92M | 81.00 | 78.41 | 82.24 | 87.65  | 77.99 | 91.58 | 70.15 | 88.12 | 82.14        |
|             | Aurora ( $r = 2$ )                  | 1.18M | 76.20 | 77.13 | 72.93 | 84.28  | 73.08 | 89.73 | 67.77 | 82.45 | 77.95        |
|             | Aurora ( $r = 8$ )                  | 4.72M | 81.60 | 78.50 | 82.08 | 87.27  | 77.48 | 91.62 | 70.46 | 88.05 | 82.13        |
|             | <b>GenLoRA</b> ( $r = 8, g = 16$ )  | 0.98M | 85.60 | 79.01 | 84.85 | 88.57  | 79.38 | 91.75 | 71.83 | 91.45 | <u>84.05</u> |
| Gemma-7B    | <b>GenLoRA</b> ( $r = 32, g = 16$ ) | 2.16M | 86.80 | 80.12 | 85.71 | 88.74  | 80.91 | 91.37 | 72.63 | 92.87 | <b>84.89</b> |
|             | LoRA ( $r = 8$ )                    | 4.82M | 81.80 | 82.76 | 86.19 | 88.30  | 77.99 | 92.55 | 68.84 | 91.16 | 83.70        |
|             | MELoRA ( $r = 8$ )                  | 4.82M | 79.60 | 79.86 | 78.61 | 84.93  | 74.67 | 89.73 | 69.27 | 87.81 | 80.56        |
|             | HiRA ( $r = 8$ )                    | 4.82M | 85.80 | 83.45 | 85.00 | 88.30  | 77.94 | 93.14 | 69.66 | 92.31 | 84.45        |
|             | DoRA ( $r = 8$ )                    | 5.16M | 82.60 | 80.89 | 84.06 | 85.47  | 75.95 | 91.16 | 69.20 | 89.42 | 82.34        |
|             | Aurora ( $r = 2$ )                  | 1.20M | 80.00 | 81.48 | 79.24 | 85.75  | 75.90 | 90.57 | 68.13 | 85.63 | 80.84        |
|             | Aurora ( $r = 8$ )                  | 4.82M | 82.40 | 82.76 | 83.50 | 85.96  | 76.82 | 91.75 | 70.28 | 90.08 | 82.94        |
| Qwen2.5-14B | <b>GenLoRA</b> ( $r = 8, g = 8$ )   | 0.77M | 84.80 | 80.80 | 86.90 | 87.54  | 77.43 | 92.26 | 71.25 | 92.07 | 84.13        |
|             | <b>GenLoRA</b> ( $r = 16, g = 8$ )  | 0.95M | 88.00 | 84.64 | 88.48 | 89.23  | 81.53 | 94.19 | 70.95 | 94.19 | <b>86.40</b> |
|             | LoRA ( $r = 8$ )                    | 8.65M | 93.00 | 92.66 | 84.85 | 91.89  | 81.47 | 97.35 | 74.71 | 95.33 | 88.91        |
|             | MELoRA ( $r = 8$ )                  | 8.65M | 90.40 | 91.30 | 77.19 | 90.75  | 79.79 | 97.10 | 72.54 | 92.91 | 86.50        |
|             | HiRA ( $r = 8$ )                    | 8.65M | 94.20 | 93.26 | 89.98 | 93.09  | 83.88 | 97.98 | 75.87 | 96.50 | 90.60        |
|             | DoRA ( $r = 8$ )                    | 8.99M | 93.20 | 92.75 | 84.85 | 92.00  | 81.73 | 97.35 | 74.71 | 95.37 | 88.99        |
|             | Aurora ( $r = 2$ )                  | 2.16M | 90.60 | 91.21 | 78.22 | 90.86  | 80.19 | 97.05 | 73.49 | 93.81 | 86.93        |
| LLaMA-3-8B  | Aurora ( $r = 8$ )                  | 8.65M | 92.60 | 92.66 | 84.85 | 91.89  | 81.58 | 97.39 | 74.62 | 95.33 | 88.86        |
|             | <b>GenLoRA</b> ( $r = 8, g = 8$ )   | 1.38M | 94.80 | 93.60 | 91.08 | 92.98  | 84.24 | 97.77 | 76.39 | 96.25 | <u>90.80</u> |
|             | <b>GenLoRA</b> ( $r = 32, g = 8$ )  | 2.26M | 94.80 | 94.20 | 90.77 | 93.31  | 84.44 | 98.11 | 76.79 | 96.36 | <b>91.10</b> |

Table 3. The performance on Code Generation tasks (HumanEval+) with LLaMA-3-8B fine-tuned on Magicoder-Evol-Instruct-110k.

| Method     | #Params                             | Train Time | Relative Time | Pass@1        | Pass@5       | Pass@10      |              |
|------------|-------------------------------------|------------|---------------|---------------|--------------|--------------|--------------|
| LLaMA-3-8B | LoRA ( $r = 8$ )                    | 4.72M      | 11.6h         | 1.00 $\times$ | 20.79        | 35.48        | 41.31        |
|            | MELoRA ( $r = 8$ )                  | 4.72M      | 10.3h         | 0.88 $\times$ | 17.41        | 26.99        | 31.53        |
|            | HiRA ( $r = 8$ )                    | 4.72M      | 10.6h         | 0.91 $\times$ | 25.33        | 35.36        | 39.72        |
|            | DoRA ( $r = 8$ )                    | 4.92M      | 11.9h         | 1.03 $\times$ | 17.01        | 31.37        | 37.36        |
|            | Aurora ( $r = 2$ )                  | 1.18M      | 11.1h         | 0.96 $\times$ | 21.4         | 33.12        | 38.28        |
|            | Aurora ( $r = 8$ )                  | 4.72M      | 11.8h         | 1.02 $\times$ | 17.15        | 32.11        | 38.32        |
|            | <b>GenLoRA</b> ( $r = 8, g = 16$ )  | 0.98M      | 11.7h         | 1.01 $\times$ | <u>25.42</u> | <u>36.36</u> | <u>41.48</u> |
| LLaMA-3-8B | <b>GenLoRA</b> ( $r = 32, g = 16$ ) | 2.16M      | 12.2h         | 1.05 $\times$ | <b>28.30</b> | <b>41.92</b> | <b>47.77</b> |

Table 4. Ablation study on the components of GenLoRA. The parameter count is kept consistent at 0.98M for fair comparison.

| Method                                 | #Params | Avg          |
|--|---------|--------------|
| GenLoRA( $r = 8, g = 16$ )             | 0.98M   | <b>70.17</b> |
| GenLoRA( $r = 8, g = 16$ ) w.o. Norm   | 0.98M   | 63.21        |
| GenLoRA( $r = 128, g = 1$ ) w.o. Group | 0.98M   | 66.05        |

wise Normalization and Group-wise Decomposition. To ensure a fair comparison, the parameter count was maintained at approximately 0.98M across all variants.

As shown in Table 4, removing normalization leads to a sharp performance decline from 70.17% to 63.21%. We attribute this to the uncontrolled distribution of grid inputs; without normalization, inputs tend to cluster within a narrow range, falling into largely identical grids. This concentration prevents the model from utilizing the full grid resolution,

rendering the RBF fitting capability ineffective.

Regarding the grouping strategy, we compared our default setting ( $g = 16, r = 8$ ) against a non-grouped variant ( $g = 1$ ) with an increased rank ( $r = 128$ ) to match the parameter budget. The results show that the non-grouped version lags significantly behind. This demonstrates that simply expanding the rank is less effective than our grouping mechanism. Specifically, the group-wise decomposition enhances the non-linear fitting capability by avoiding RBF functions fitting higher-dimensional data, providing a structural advantage that outweighs raw rank increase.

#### 4.4. Scalability Analysis

We evaluate the scalability of GenLoRA on mathematical reasoning tasks using LLaMA3-8B from three perspectives: the LoRA rank, the group size, and the tuning granularity.

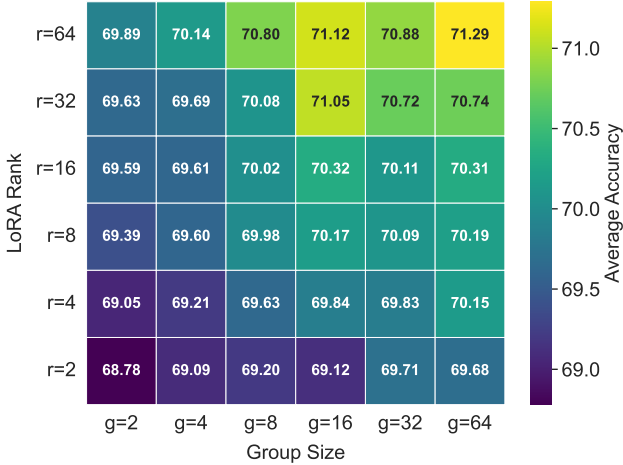


Figure 3. Accuracy of GenLoRA at varying ranks and group sizes.

Table 5. Accuracy of LoRA ( $r = 8$ ) and GenLoRA ( $r = 8, g = 16$ ) across different tuning granularities on LLaMA3-8B.

| Method  | Q            | QV           | QKV          | QKVUD        | QKVOGUD      |
|---------|--------------|--------------|--------------|--------------|--------------|
| LoRA    | 64.88        | 67.46        | 67.87        | 71.19        | 72.02        |
| GenLoRA | <b>68.59</b> | <b>69.91</b> | <b>71.05</b> | <b>72.07</b> | <b>73.08</b> |

**Impact of Rank and Group Size.** We investigate the interaction between rank ( $r$ ) and group size ( $g$ ) by varying both within  $\{2, 4, 8, 16, 32, 64\}$ , as visualized in Figure 3. Generally, increasing  $r$  and  $g$  enhances model capacity. However, we observe that the performance gains tend to stabilize around  $g = 16$ ; further increasing the group size does not yield significant improvements. We believe that this is because the fitting capability of the non-linear functions has approached its limit.

**Impact of Tuning Granularity.** Finally, we evaluate the scalability of GenLoRA under different tuning granularities. We introduce five distinct settings: Q, QV, QKV, QKVUD, and QKVOGUD, where Q, K, and V denote the query, key, and value projection weights, and O, G, U, and D represent the output, gate, up, and down projection weights, respectively. As shown in Table 5, GenLoRA consistently outperforms LoRA across all configurations. Most notably, in the most restricted setting (Q), GenLoRA surpasses LoRA by a significant margin of 3.71%, highlighting its superior efficiency in feature extraction. With comprehensive tuning (QKVOGUD), GenLoRA scales effectively to a peak accuracy of 73.08%, maintaining its robust lead over LoRA.

#### 4.5. Singular Value Analysis

To investigate whether GenLoRA effectively utilizes its expanded rank capacity, we analyze the distribution of singular values of the weight updates in Figure 4. The left panel reveals that while both LoRA and GenLoRA exhibit effective

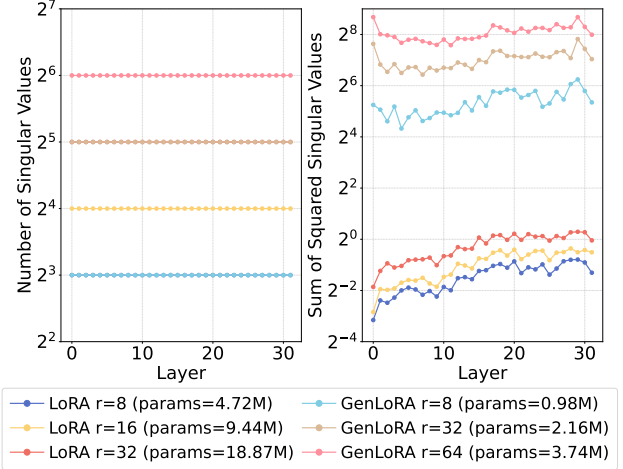


Figure 4. Singular value analysis of Query layers. (Left) Number of singular values  $> 0.005$ . (Right) Sum of squared singular values. In the left plot, LoRA and GenLoRA with  $r = \{8, 32\}$  overlap, resulting in only the GenLoRA colors being visible.

ranks equal to their preset configurations, GenLoRA enables significantly higher rank with fewer trainable parameters. In particular, GenLoRA ( $r = 64$ ) attains a full effective rank of 64 using only 3.74M parameters, representing an increase in capacity 8 $\times$  over LoRA with a higher parameter ( $r = 8, 4.72\text{M}$ ). This confirms that the synthesized ranks are non-degenerate and contribute to enhancing model capacity.

Furthermore, the sum of squared singular values (Right) measures the total contribution of all singular modes of the weight matrices. It reflects how much feature variation the matrices can express and corroborates this observation. GenLoRA exhibits a substantially higher sum of squared singular values than LoRA across all layers. Notably, GenLoRA ( $r = 8$ ) displays significantly higher energy than LoRA ( $r = 32$ ), demonstrating GenLoRA captures more significant feature variations with a fraction of parameters.

## 5. Conclusion

In this paper, we analyze the parameter efficiency of LoRA from the perspective of basis vector redundancy. Our analysis reveals that standard LoRA suffers from inefficiency due to the explicit storage of high-dimensional vectors. To address this, we propose Generative Low-Rank Adapter (GenLoRA), which replaces explicit matrix storage with synthesis. GenLoRA constructs basis vectors via lightweight Radial Basis Functions (RBFs) from shared latent vectors, thereby enabling high-rank adaptation with minimal parameter overhead. Extensive experiments demonstrate that GenLoRA outperforms LoRA and its variants across diverse tasks. Notably, GenLoRA achieves a 2–4% improvement on natural language generation and 6–8% on code generation, while utilizing significantly fewer parameters.

## Impact Statement

This paper introduces GenLoRA, a parameter-efficient fine-tuning framework that utilizes non-linear functions to synthesize low-rank adaptation weights. Our work builds upon existing efficient fine-tuning paradigms to enhance model scalability and efficiency, and we assert that it does not introduce any negative social implications or ethical concerns that would necessitate further discussion.

## References

Allal, L. B., Muennighoff, N., Umapathi, L. K., Lipkin, B., and Von Werra, L. A framework for the evaluation of code generation models, 2022.

Baker Jr, G. A. The theory and application of the padé approximant method. Technical report, Los Alamos Scientific Lab., Univ. of California, N. Mex., 1963.

Bisk, Y., Zellers, R., Gao, J., Choi, Y., et al. Piqa: Reasoning about physical commonsense in natural language. In *Proceedings of the AAAI conference on artificial intelligence*, volume 34, pp. 7432–7439, 2020.

Buhmann, M. D. Radial basis functions. *Acta numerica*, 9: 1–38, 2000.

Cai, Z., Cao, M., Chen, H., Chen, K., Chen, K., Chen, X., Chen, X., Chen, Z., Chen, Z., Chu, P., et al. Internlm2 technical report. *arXiv preprint arXiv:2403.17297*, 2024.

Clark, C., Lee, K., Chang, M.-W., Kwiatkowski, T., Collins, M., and Toutanova, K. Boolq: Exploring the surprising difficulty of natural yes/no questions. *arXiv preprint arXiv:1905.10044*, 2019.

Clark, P., Cowhey, I., Etzioni, O., Khot, T., Sabharwal, A., Schoenick, C., and Tafjord, O. Think you have solved question answering? try arc, the ai2 reasoning challenge. *arXiv preprint arXiv:1803.05457*, 2018.

Cobbe, K., Kosaraju, V., Bavarian, M., Chen, M., Jun, H., Kaiser, L., Plappert, M., Tworek, J., Hilton, J., Nakano, R., et al. Training verifiers to solve math word problems. *arXiv preprint arXiv:2110.14168*, 2021.

De Boor, C. On calculating with b-splines. *Journal of Approximation theory*, 6(1):50–62, 1972.

DeepSeek, A., Liu, A., Feng, B., Xue, B., Wang, B., Wu, B., Lu, C., Zhao, C., Deng, C., Zhang, C., et al. Deepseek-v3 technical report. *arXiv preprint arXiv:2412.19437*, 2024.

Dong, H., Zhu, W., Song, G., and Wang, L. Aurora: Breaking low-rank bottleneck of lora with nonlinear mapping. *arXiv preprint arXiv:2505.18738*, 2025.

Dubey, A., Jauhri, A., Pandey, A., Kadian, A., Al-Dahle, A., Letman, A., Mathur, A., Schelten, A., Yang, A., Fan, A., et al. The llama 3 herd of models. *arXiv e-prints*, pp. arXiv–2407, 2024.

Edalati, A., Tahaei, M., Kobyzev, I., Nia, V. P., Clark, J. J., and Rezagholizadeh, M. Krona: Parameter-efficient tuning with kronecker adapter. In *Enhancing LLM Performance: Efficacy, Fine-Tuning, and Inference Techniques*, pp. 49–65. Springer, 2025.

Edmunds, D. E., Gurka, P., and Lang, J. Properties of generalized trigonometric functions. *Journal of Approximation Theory*, 164(1):47–56, 2012.

Gao, Z., Wang, Q., Chen, A., Liu, Z., Wu, B., Chen, L., and Li, J. Parameter-efficient fine-tuning with discrete fourier transform. *arXiv preprint arXiv:2405.03003*, 2024.

Hayou, S., Ghosh, N., and Yu, B. Lora+: Efficient low rank adaptation of large models. *arXiv preprint arXiv:2402.12354*, 2024.

He, K., Zhang, X., Ren, S., and Sun, J. Delving deep into rectifiers: Surpassing human-level performance on imagenet classification. In *Proceedings of the IEEE international conference on computer vision*, pp. 1026–1034, 2015.

Hosseini, M. J., Hajishirzi, H., Etzioni, O., and Kushman, N. Learning to solve arithmetic word problems with verb categorization. In *Proceedings of the 2014 Conference on Empirical Methods in Natural Language Processing (EMNLP)*, pp. 523–533, 2014.

Houlsby, N., Giurgiu, A., Jastrzebski, S., Morrone, B., De Laroussilhe, Q., Gesmundo, A., Attariyan, M., and Gelly, S. Parameter-efficient transfer learning for nlp. In *International conference on machine learning*, pp. 2790–2799. PMLR, 2019.

Hu, E. J., Shen, Y., Wallis, P., Allen-Zhu, Z., Li, Y., Wang, S., Wang, L., Chen, W., et al. Lora: Low-rank adaptation of large language models. *ICLR*, 1(2):3, 2022.

Hu, Z., Wang, L., Lan, Y., Xu, W., Lim, E.-P., Bing, L., Xu, X., Poria, S., and Lee, R. Llm-adapters: An adapter family for parameter-efficient fine-tuning of large language models. In *Proceedings of the 2023 conference on empirical methods in natural language processing*, pp. 5254–5276, 2023.

Huang, Q., Ko, T., Zhuang, Z., Tang, L., and Zhang, Y. Hira: Parameter-efficient hadamard high-rank adaptation for large language models. In *The Thirteenth International Conference on Learning Representations*, 2025.

Ji, Y., Saratchandran, H., Gordon, C., Zhang, Z., and Lucey, S. Efficient learning with sine-activated low-rank matrices. *arXiv preprint arXiv:2403.19243*, 2024.

Koncel-Kedziorski, R., Hajishirzi, H., Sabharwal, A., Etzioni, O., and Ang, S. D. Parsing algebraic word problems into equations. *Trans. Assoc. Comput. Linguistics*, 3:585–597, 2015. doi: 10.1162/TACL\_A\_00160. URL [https://doi.org/10.1162/tacl\\_a\\_00160](https://doi.org/10.1162/tacl_a_00160).

Koohpayegani, S. A., Navaneet, K., Nooralinejad, P., Kolouri, S., and Pirsavash, H. Nola: Compressing lora using linear combination of random basis. *arXiv preprint arXiv:2310.02556*, 2023.

Langley, P. Crafting papers on machine learning. In Langley, P. (ed.), *Proceedings of the 17th International Conference on Machine Learning (ICML 2000)*, pp. 1207–1216, Stanford, CA, 2000. Morgan Kaufmann.

Lester, B., Al-Rfou, R., and Constant, N. The power of scale for parameter-efficient prompt tuning. *arXiv preprint arXiv:2104.08691*, 2021.

Li, M., Chen, J., Feng, W., Li, B., Dai, F., Zhao, S., and He, Q. Hyperlora: Parameter-efficient adaptive generation for portrait synthesis. In *Proceedings of the Computer Vision and Pattern Recognition Conference*, pp. 13114–13123, 2025a.

Li, S., Luo, X., Wang, H., Tang, X., Cui, Z., Liu, D., Li, Y., He, X., and Li, R. Beyond higher rank: Token-wise input-output projections for efficient low-rank adaptation. *arXiv preprint arXiv:2510.23123*, 2025b.

Li, Y., Song, L., and Hou, H. Loran: Improved low-rank adaptation by a non-linear transformation. In *Findings of the Association for Computational Linguistics: EMNLP 2024*, pp. 3134–3143, 2024.

Ling, W., Yogatama, D., Dyer, C., and Blunsom, P. Program induction by rationale generation: Learning to solve and explain algebraic word problems. *arXiv preprint arXiv:1705.04146*, 2017.

Liu, S.-Y., Wang, C.-Y., Yin, H., Molchanov, P., Wang, Y.-C. F., Cheng, K.-T., and Chen, M.-H. Dora: Weight-decomposed low-rank adaptation. In *Forty-first International Conference on Machine Learning*, 2024a.

Liu, Z., Wang, Y., Vaidya, S., Ruehle, F., Halverson, J., Soljačić, M., Hou, T. Y., and Tegmark, M. Kan: Kolmogorov-arnold networks. *arXiv preprint arXiv:2404.19756*, 2024b.

Loshchilov, I. and Hutter, F. Decoupled weight decay regularization. *arXiv preprint arXiv:1711.05101*, 2017.

Luo, Z., Xu, C., Zhao, P., Sun, Q., Geng, X., Hu, W., Tao, C., Ma, J., Lin, Q., and Jiang, D. Wizardcoder: Empowering code large language models with evol-instruct. *arXiv preprint arXiv:2306.08568*, 2023.

Meng, F., Wang, Z., and Zhang, M. Pissa: Principal singular values and singular vectors adaptation of large language models. *Advances in Neural Information Processing Systems*, 37:121038–121072, 2024.

Mihaylov, T., Clark, P., Khot, T., and Sabharwal, A. Can a suit of armor conduct electricity? a new dataset for open book question answering. *arXiv preprint arXiv:1809.02789*, 2018.

Park, J. and Sandberg, I. W. Universal approximation using radial-basis-function networks. *Neural computation*, 3 (2):246–257, 1991.

Patel, A., Bhattacharya, S., and Goyal, N. Are NLP models really able to solve simple math word problems? In Toutanova, K., Rumshisky, A., Zettlemoyer, L., Hakkani-Tür, D., Beltagy, I., Bethard, S., Cotterell, R., Chakraborty, T., and Zhou, Y. (eds.), *Proceedings of the 2021 Conference of the North American Chapter of the Association for Computational Linguistics: Human Language Technologies, NAACL-HLT 2021, Online, June 6-11, 2021*, pp. 2080–2094. Association for Computational Linguistics, 2021. doi: 10.18653/V1/2021.NAACL-MAIN.168. URL <https://doi.org/10.18653/v1/2021.naacl-main.168>.

Ren, P., Shi, C., Wu, S., Zhang, M., Ren, Z., de Rijke, M., Chen, Z., and Pei, J. Melora: Mini-ensemble low-rank adapters for parameter-efficient fine-tuning. *arXiv preprint arXiv:2402.17263*, 2024.

Roy, S. and Roth, D. Solving general arithmetic word problems. *CoRR*, abs/1608.01413, 2016. URL <http://arxiv.org/abs/1608.01413>.

Sakaguchi, K., Bras, R. L., Bhagavatula, C., and Choi, Y. Winogrande: An adversarial winograd schema challenge at scale. *Communications of the ACM*, 64(9):99–106, 2021.

Sap, M., Rashkin, H., Chen, D., LeBras, R., and Choi, Y. Socialqa: Commonsense reasoning about social interactions. *arXiv preprint arXiv:1904.09728*, 2019.

Team, G., Mesnard, T., Hardin, C., Dadashi, R., Bhupatiraju, S., Pathak, S., Sifre, L., Rivière, M., Kale, M. S., Love, J., et al. Gemma: Open models based on gemini research and technology. *arXiv preprint arXiv:2403.08295*, 2024.

Wang, S., Yu, L., and Li, J. Lora-ga: Low-rank adaptation with gradient approximation. *Advances in Neural Information Processing Systems*, 37:54905–54931, 2024.

Wei, Y., Wang, Z., Liu, J., Ding, Y., and Zhang, L. Magi-coder: Empowering code generation with oss-instruct. *arXiv preprint arXiv:2312.02120*, 2023.

Yang, A., Yang, B., Zhang, B., Hui, B., Zheng, B., Yu, B., Li, C., Liu, D., Huang, F., Wei, H., Lin, H., Yang, J., Tu, J., Zhang, J., Yang, J., Yang, J., Zhou, J., Lin, J., Dang, K., Lu, K., Bao, K., Yang, K., Yu, L., Li, M., Xue, M., Zhang, P., Zhu, Q., Men, R., Lin, R., Li, T., Xia, T., Ren, X., Ren, X., Fan, Y., Su, Y., Zhang, Y., Wan, Y., Liu, Y., Cui, Z., Zhang, Z., and Qiu, Z. Qwen2.5 technical report. *CoRR*, abs/2412.15115, 2024. doi: 10.48550/ARXIV.2412.15115. URL <https://doi.org/10.48550/arXiv.2412.15115>.

Yin, B., Yang, X., and Wang, X. Don't forget the nonlinearity: Unlocking activation functions in efficient fine-tuning. *arXiv preprint arXiv:2509.13240*, 2025.

Zellers, R., Holtzman, A., Bisk, Y., Farhadi, A., and Choi, Y. Hellaswag: Can a machine really finish your sentence? *arXiv preprint arXiv:1905.07830*, 2019.

Zhang, Q., Chen, M., Bukharin, A., Karampatziakis, N., He, P., Cheng, Y., Chen, W., and Zhao, T. Adalora: Adaptive budget allocation for parameter-efficient fine-tuning. *arXiv preprint arXiv:2303.10512*, 2023.

## A. Proof of Rank Boundedness

In this appendix, we provide the theoretical analysis for Proposition 3.1. We formally demonstrate that the algebraic structure of the GenLoRA update, constructed via generator functions, strictly adheres to the low-rank constraint.

**Proposition 3.1 (Restated).** *Let  $\Delta W_{\text{Gen}} \in \mathbb{R}^{m \times n}$  be the weight update generated by GenLoRA with  $r$  pairs of generator functions  $\{f_i^B\}_{i=1}^r$  and  $\{f_i^A\}_{i=1}^r$ , where  $r \ll \min(m, n)$ . The rank of the update matrix satisfies:*

$$\text{rank}(\Delta W_{\text{Gen}}) \leq r. \quad (12)$$

First, we establish the algebraic form of the update. Given latent vectors  $Z_B, Z_A$  and generator parameters  $\Theta$ , the instantiated basis vectors for  $i \in \{1, \dots, r\}$  are  $b_i = f_i^B(Z_B) \in \mathbb{R}^m$  and  $a_i = f_i^A(Z_A) \in \mathbb{R}^n$ . The GenLoRA update is defined as the summation of outer products:  $\Delta W_{\text{Gen}} = \sum_{i=1}^r b_i a_i^\top$ .

**Lemma A.1.** *The summation of outer products  $\sum_{i=1}^r b_i a_i^\top$  is algebraically equivalent to the matrix product  $BA$ , where  $B = [b_1, \dots, b_r]$  and  $A = [a_1, \dots, a_r]^\top$ .*

*Proof.* We verify this equality using element-wise index notation. Let  $(M)_{jk}$  denote the entry of a matrix  $M$  at the  $j$ -th row and  $k$ -th column. Compute the element  $(BA)_{jk}$ :

$$(BA)_{jk} = \sum_{p=1}^r (B)_{jp} (A)_{pk}. \quad (13)$$

By construction, the  $p$ -th column of  $B$  is  $b_p$ , so  $(B)_{jp} = (b_p)_j$ . The  $p$ -th row of  $A$  is  $a_p^\top$ , so  $(A)_{pk} = (a_p)_k$ . Substituting these terms:

$$(BA)_{jk} = \sum_{p=1}^r (b_p)_j (a_p)_k. \quad (14)$$

Now, compute the element of the summation term. The  $(j, k)$ -th entry of the outer product  $b_i a_i^\top$  is  $(b_i)_j (a_i)_k$ . Summing over  $i = 1$  to  $r$ :

$$\left( \sum_{i=1}^r b_i a_i^\top \right)_{jk} = \sum_{i=1}^r (b_i)_j (a_i)_k. \quad (15)$$

Since the element-wise expressions are identical for all  $j, k$ , it follows that  $\Delta W_{\text{Gen}} = BA$ .  $\square$

**Lemma A.2.** *The rank of the factorized matrix product  $BA$  is bounded by  $r$ .*

*Proof.* Recall that the rank of a matrix corresponds to the dimension of its column space. The column space of the product  $BA$ , denoted  $\mathcal{C}(BA)$ , is defined as:

$$\mathcal{C}(BA) = \{B(Av) \mid v \in \mathbb{R}^n\}. \quad (16)$$

Since  $Av$  is a vector in  $\mathbb{R}^r$ , let  $u = Av$ . Then  $\mathcal{C}(BA) \subseteq \{Bu \mid u \in \mathbb{R}^r\} = \mathcal{C}(B)$ . Consequently, the dimension of the column space of  $BA$  cannot exceed the dimension of the column space of  $B$ :

$$\text{rank}(BA) \leq \text{rank}(B). \quad (17)$$

The matrix  $B \in \mathbb{R}^{m \times r}$  has exactly  $r$  columns. The rank of a matrix is bounded by the number of its columns, so  $\text{rank}(B) \leq \min(m, r)$ . Given the low-rank setting where  $r < m$ , we have  $\text{rank}(B) \leq r$ . Therefore,  $\text{rank}(\Delta W_{\text{Gen}}) = \text{rank}(BA) \leq r$ .  $\square$

**Conclusion.** From Lemma A.1, the update  $\Delta W_{\text{Gen}}$  is equivalent to the matrix product  $BA$ . From Lemma A.2, the rank of this product is at most  $r$ . Thus, Proposition 3.1 holds.

## B. Proof of Gradient Boundedness

In this appendix, we provide the complete theoretical analysis for Proposition 3.2. We demonstrate that the gradients of the loss function with respect to both the latent vectors and the generator parameters are strictly bounded.

**Proposition 3.2 (Restated).** *In GenLoRA, the gradients of the loss function  $\mathcal{L}$  with respect to the latent vectors  $Z_A, Z_B$  and generator weights  $\Theta_A, \Theta_B$  are locally bounded. That is, for any bounded parameter set, there exist constants  $C_1, C_2 > 0$  such that*

$$\left\| \frac{\partial \mathcal{L}}{\partial Z} \right\| < C_1, \quad \left\| \frac{\partial \mathcal{L}}{\partial \Theta} \right\| < C_2. \quad (18)$$

**Lemma B.1.** *The gradients of the loss function with respect to the generator weights  $\Theta$  are locally bounded.*

*Proof.* The parameter set  $\Theta$  consists of the RBF weights  $\{w_k\}$  and the base linear weight  $w_{\text{base}}$ . We analyze them respectively.

For  $w_k$ , by the chain rule,

$$\frac{\partial \mathcal{L}}{\partial w_k} = \frac{\partial \mathcal{L}}{\partial \Delta W_{\text{Gen}}} \cdot \frac{\partial \Delta W_{\text{Gen}}}{\partial \phi} \cdot \frac{\partial \phi(\hat{x})}{\partial w_k}.$$

Since  $\frac{\partial \phi(\hat{x})}{\partial w_k} = \varphi_k(\hat{x}) = \exp\left(-\left(\frac{\hat{x}-\mu_k}{h}\right)^2\right)$  and the Gaussian basis satisfies  $0 < \varphi_k(\hat{x}) \leq 1$  for all  $\hat{x} \in \mathbb{R}$ , this term is uniformly bounded.

For  $w_{\text{base}}$ ,

$$\frac{\partial \phi(\hat{x})}{\partial w_{\text{base}}} = \sigma(\hat{x}),$$

where  $\sigma(\cdot)$  denotes the SiLU activation. Although  $\sigma(\hat{x})$  is unbounded, the gradient with respect to  $w_{\text{base}}$  is evaluated at a fixed  $\hat{x}$  during backpropagation. Assuming the loss gradient  $\frac{\partial \mathcal{L}}{\partial \Delta W_{\text{Gen}}}$  is bounded, which holds for standard losses and finite network outputs, it follows that for any bounded parameter set  $\Theta \in \mathcal{B}$ , both  $\frac{\partial \mathcal{L}}{\partial w_k}$  and  $\frac{\partial \mathcal{L}}{\partial w_{\text{base}}}$  are bounded.

Therefore, the gradient  $\frac{\partial \mathcal{L}}{\partial \Theta}$  is locally bounded.  $\square$

**Lemma B.2.** *The gradients of the loss function with respect to the latent vectors  $Z$  are locally bounded.*

*Proof.* Let  $z$  be an element of the latent vector  $Z$ . Compute the gradient  $\frac{\partial \mathcal{L}}{\partial z}$ :

$$\frac{\partial \mathcal{L}}{\partial z} = \frac{\partial \mathcal{L}}{\partial \Delta W_{\text{Gen}}} \cdot \frac{\partial \Delta W_{\text{Gen}}}{\partial \phi} \cdot \frac{\partial \phi(\hat{x})}{\partial \hat{x}} \cdot \frac{\partial \hat{x}}{\partial z}. \quad (19)$$

We analyze the partial derivatives  $\frac{\partial \phi}{\partial \hat{x}}$  and  $\frac{\partial \hat{x}}{\partial z}$  in turn.

Compute  $\frac{\partial \phi(\hat{x})}{\partial \hat{x}}$ :

$$\frac{\partial \phi(\hat{x})}{\partial \hat{x}} = w_{\text{base}} \sigma'(\hat{x}) + \sum_{k=1}^K w_k \varphi'_k(\hat{x}). \quad (20)$$

The derivative of the SiLU activation  $\sigma'(t)$  is globally bounded. The derivative of the Gaussian basis is given by  $\varphi'_k(\hat{x}) = -2 \frac{(\hat{x}-\mu_k)}{h^2} \varphi_k(\hat{x})$ , where the function  $g(u) = ue^{-u^2}$  is globally bounded. Therefore, both  $\sigma'(\cdot)$  and  $\varphi'_k(\cdot)$  are bounded functions. Conditioning on finite generator parameters  $(w_{\text{base}}, \{w_k\})$  at the current optimization step,  $\frac{\partial \phi(\hat{x})}{\partial \hat{x}}$  is bounded as a finite linear combination of bounded functions.

Compute  $\frac{\partial \hat{x}}{\partial z}$ : From Eq. (6), the instance-wise normalized variable is defined as

$$\hat{x}_i = \frac{z_i - \mu}{\sigma + \varepsilon}, \quad (21)$$

where

$$\mu = \frac{1}{n} \sum_{k=1}^n z_k, \quad \sigma = \sqrt{\frac{1}{n} \sum_{k=1}^n (z_k - \mu)^2}, \quad (22)$$

both of which depend on the latent vector  $z$ .

We rewrite  $\hat{x}_i$  as a product

$$\hat{x}_i = (z_i - \mu)(\sigma + \varepsilon)^{-1}, \quad (23)$$

and apply the chain rule with respect to  $z_j$ :

$$\frac{\partial \hat{x}_i}{\partial z_j} = \frac{1}{\sigma + \varepsilon} \frac{\partial(z_i - \mu)}{\partial z_j} + (z_i - \mu) \frac{\partial(\sigma + \varepsilon)^{-1}}{\partial z_j}. \quad (24)$$

We first compute the derivative of the numerator. Since  $\mu = \frac{1}{n} \sum_{k=1}^n z_k$ , it follows that

$$\frac{\partial(z_i - \mu)}{\partial z_j} = \delta_{ij} - \frac{1}{n}, \quad (25)$$

where  $\delta_{ij}$  denotes the Kronecker delta.

Next, we compute the derivative of the inverse standard deviation term. Let  $\sigma^2 = \frac{1}{n} \sum_{k=1}^n (z_k - \mu)^2$ . Differentiating with respect to  $z_j$  yields

$$\frac{\partial \sigma^2}{\partial z_j} = \frac{2}{n} (z_j - \mu), \quad (26)$$

and thus

$$\frac{\partial \sigma}{\partial z_j} = \frac{z_j - \mu}{n \sigma}. \quad (27)$$

Applying the chain rule again, we obtain

$$\frac{\partial(\sigma + \varepsilon)^{-1}}{\partial z_j} = -\frac{1}{(\sigma + \varepsilon)^2} \frac{\partial \sigma}{\partial z_j} = -\frac{z_j - \mu}{n \sigma (\sigma + \varepsilon)^2}. \quad (28)$$

Substituting the above results back, the Jacobian element is given by

$$\frac{\partial \hat{x}_i}{\partial z_j} = \frac{1}{\sigma + \varepsilon} \left( \delta_{ij} - \frac{1}{n} - \frac{(z_i - \mu)(z_j - \mu)}{n \sigma (\sigma + \varepsilon)} \right). \quad (29)$$

Due to the presence of the stability constant  $\varepsilon > 0$  and the assumption that the latent vector  $z$  has finite second moments, each term in the above expression is bounded. Therefore, the operator norm of the Jacobian  $\frac{\partial \hat{x}}{\partial z}$  is bounded. and by the chain rule,  $\frac{\partial \mathcal{L}}{\partial z}$  is bounded as it is a product of bounded terms, and there exists a constant  $C_1 > 0$  such that, for any bounded parameter set,  $\left\| \frac{\partial \mathcal{L}}{\partial z} \right\| < C_1$ .

□

## C. Algorithmic Complexity Analysis

In this section, we provide a theoretical comparison between Radial Basis Functions (RBFs) and B-Spline from an algorithmic perspective. We analyze why RBFs constitute a more efficient choice for the high-dimensional generation tasks in GenLoRA.

### C.1. Computational Operations

**RBFs: Single-Step Global Mapping** The RBF generator models nonlinearity via a unified, single-step calculation that is inherently parallelizable. For a given input  $x$  and a grid resolution  $N$  (denoting the number of basis functions),

the algorithm executes three fundamental operations: distance calculation ( $(x - \mu_k)^2$ ), Gaussian activation ( $\exp(\cdot)$ ), and weighted aggregation. Crucially, these operations are strictly independent across the grid dimension  $N$ , meaning there are no data dependencies between the  $k$ -th and  $(k + 1)$ -th basis functions. Consequently, the entire process can be fused and expressed as a single vectorized matrix operation. In terms of sequential complexity, this represents an  $\mathcal{O}(1)$  depth algorithm, regardless of the grid size, making it exceptionally efficient on modern SIMD architectures like GPUs.

**B-Spline: Recursive Dependency** B-Splines are defined by the Cox-de Boor recursion algorithm, which inherently requires an iterative computation process. A spline of order  $k$  (degree  $k - 1$ ) is computed by recursively evaluating basis functions from order 0 up to  $k$ . This process begins with an initialization step to locate the input  $x$  within the knot vector intervals. Subsequently, the algorithm enters a recursive loop of depth  $k$ , where at each depth  $d \in [1, k]$ , the value of a basis function is derived via linear interpolation of two basis functions from the previous depth  $d - 1$ . While the total operation count scales as  $\mathcal{O}(k^2)$ , the primary computational bottleneck is the requirement for  $\mathcal{O}(k)$  sequential iterations to resolve these dependencies. Unlike RBFs, B-Splines impose strict sequential constraints: the basis values at step  $d$  cannot be computed until step  $d - 1$  is fully resolved, which significantly limits the potential for operator fusion and parallel execution.

## C.2. Space and Gradient Complexity

In deep learning, the training memory cost is dominated by the requirement to store intermediate activations for gradient computation. For RBF generators, the computational graph is shallow, necessitating the backpropagation engine to trace through only a single exponential layer. Consequently, the space complexity remains linear with respect to the grid resolution  $N$ , i.e.,  $\mathcal{O}(N)$ . In contrast, B-Spline generators construct an inherently deep computational graph due to their recursive definition. Since the algorithm iterates  $k$  times, the automatic differentiation engine is forced to cache intermediate basis tensors for every step of the recursion to correctly apply the chain rule. This results in a space complexity of  $\mathcal{O}(N \cdot k)$ . For high-dimensional inputs, this multiplicative factor  $k$  significantly amplifies the memory footprint during training, making B-Splines less memory-efficient than RBFs.

## C.3. Summary

Table 6 summarizes the algorithmic differences. While B-Splines offer compact support, their recursive nature and higher memory complexity for gradient computation make them less suitable for the high-throughput requirements of GenLoRA. RBFs provide a mathematically simpler and parallel-friendly alternative that aligns better with the efficiency demands of large-scale neural network training.

Table 6. Algorithmic comparison between RBF and B-Spline generators.

| Aspect                 | RBF (Ours)             | B-Spline                 |
|------------------------|------------------------|--------------------------|
| <b>Structure</b>       | Single-step Mapping    | $k$ -step Recursion      |
| <b>Dependencies</b>    | Independent (Parallel) | Sequential (Iterative)   |
| <b>Gradient Memory</b> | $\mathcal{O}(N)$       | $\mathcal{O}(N \cdot k)$ |

## D. Approximation Capability of RBF Generators

In this section, we provide the theoretical justification for the strong fitting capability of our RBF-based generators, drawing upon the fundamental mathematical properties of radial basis functions analyzed by Buhmann (2000).

### D.1. Universal Approximation Theorem

The theoretical foundation of our RBF generator is grounded in the analysis provided by Park & Sandberg (1991). We first cite the original Theorem 2 regarding the approximation capabilities of RBF networks:

**Theorem D.1** (Theorem 2 in Park & Sandberg (1991)). *Let  $K : \mathbb{R}^r \rightarrow \mathbb{R}$  be an integrable bounded function such that  $K$  is continuous almost everywhere and  $\int_{\mathbb{R}^r} K(x) dx \neq 0$ . Then the family  $S_K$  is dense in  $C(\mathbb{R}^r)$  with respect to the metric  $d$  defined by*

$$d(f, g) = \sum_{n=1}^{\infty} 2^{-n} \frac{\|(f - g) \cdot 1_{[-n, n]^r}\|_{\infty}}{1 + \|(f - g) \cdot 1_{[-n, n]^r}\|_{\infty}}. \quad (30)$$

As further explained by the authors, the statement in Theorem 2 is equivalent to the statement that  $S_K$  is uniformly dense on compacta in  $C(\mathbb{R}^r)$ . That is, for any continuous function  $f$ , any  $\epsilon > 0$ , and any compact subset  $C \subset \mathbb{R}^r$ , there exists a  $q \in S_K$  such that  $\|(q - f) \cdot 1_C\|_\infty < \epsilon$ .

## D.2. Proof of Fitting Capability in GenLoRA

We now connect the above theoretical result to the generator design in GenLoRA.

**Setup.** We model the target weight generation process as a continuous mapping  $W^* : \mathbb{R}^{d_z} \rightarrow \mathcal{W}$  from the latent space to the weight space. We emphasize that the latent vectors  $z$  are learnable parameters and are not explicitly constrained to lie in a compact domain. Accordingly, our analysis focuses on the approximation behavior of the generator when restricted to any bounded subset of the latent space, which is the standard setting for applying universal approximation results.

The generator in GenLoRA employs Gaussian radial basis functions of the form  $\phi(x) = \exp(-\|x - \mu\|^2/h^2)$ , which are integrable, bounded, continuous, and have a non-zero integral. Therefore, the kernel  $\phi$  satisfies the assumptions required in Theorem D.1.

**Approximation Result.** Let  $\mathcal{Z}_R \subset \mathbb{R}^{d_z}$  denote an arbitrary compact subset of the latent space, for example,  $\mathcal{Z}_R = \{z \in \mathbb{R}^{d_z} \mid \|z\| \leq R\}$ . Consider any scalar-valued target function  $w^*(z)$  corresponding to an element of the generated weight matrix. Since  $w^*(z)$  is continuous on the compact set  $\mathcal{Z}_R$ , by the uniform density property of Theorem D.1, for any  $\epsilon > 0$ , there exists an RBF generator  $g(z) \in S_K$  with sufficiently many basis functions such that

$$\sup_{z \in \mathcal{Z}_R} |g(z) - w^*(z)| < \epsilon. \quad (31)$$

**Conclusion.** This result establishes the expressive power of the proposed RBF-based generator in a local sense: for any bounded region of the latent space encountered during training, the generator can approximate the target weight mapping to arbitrary precision given sufficient capacity. Combined with the locally bounded gradient analysis in Appendix B, this ensures that GenLoRA admits both strong approximation capability and stable optimization behavior in practice.

## E. Algorithm Workflow

The complete training and inference workflow of GenLoRA is presented in Algorithm 1.

**Zero-Latency Inference via Weight Merging.** A critical advantage of GenLoRA is its compatibility with standard weight merging techniques. Unlike adapter methods that apply non-linearities directly to the input activation  $x$  (e.g.,  $h = W_0x + B\sigma(Ax)$ ), GenLoRA restricts non-linearity solely to the parameter generation process. Once training is complete, the latent vectors  $Z$  and generator parameters  $\Theta$  become static. Consequently, the synthesized matrices  $B$  and  $A$  evaluate to fixed constant matrices. This allows us to pre-compute the full update matrix  $\Delta W = BA$  and merge it algebraically into the pretrained weights:  $W_{\text{merged}} = W_0 + \Delta W$ . During inference, the model utilizes  $W_{\text{merged}}$  directly, incurring **zero additional computational overhead** compared to the base model.

## F. Ablation Study on Latent Vectors

In GenLoRA, the latent vectors  $Z_A$  and  $Z_B$  serve as the input ‘seeds’ for the RBF generators. A critical question is whether these vectors actively encode task-specific information or merely act as static anchors for the non-linear mapping. To investigate this, we conducted an ablation study on the LLaMA-3-8B model using the Math10K benchmark. We selectively froze the latent vectors during training while keeping the generator parameters tunable, using the GenLoRA configuration with  $r = 8$  and  $g = 16$  as the baseline.

Table 7 presents the experimental results. The standard GenLoRA, where both latent vectors are learnable, achieves an average accuracy of 70.17% with 0.98M parameters. In contrast, when we freeze both latent vectors ( $Z_A, Z_B$ ), the performance drastically drops to 60.63%, a decrease of 9.54%. This indicates that the generator functions alone are insufficient to capture the full adaptation dynamics; the optimization of the input latent space is crucial. Freezing only  $Z_A$  results in an accuracy of 62.19%. Since  $A$  determines the projection into the low-rank subspace, its rigidity likely prevents the model from extracting optimal input features. Similarly, freezing only  $Z_B$  yields an accuracy of 61.26%. As  $B$  is

**Algorithm 1** Algorithm Workflow of GenLoRA

---

**Require:** Pretrained weight  $W_0$ , Latent vectors  $Z_B, Z_A$ , RBF Generator parameters  $\Theta_B, \Theta_A$ , Training data  $\{(x_i, y_i)\}_{i=1}^N$ .

**Ensure:** Fine-tuned model weights  $W$ .

- 1: **Function** GENERATOR( $Z, \Theta$ ):
- 2:   Partition  $Z$  into groups  $\{\mathbf{x}_1, \dots, \mathbf{x}_G\}$ ; {Group-wise Decomposition}
- 3:   **for** each group  $g \in \{1, \dots, G\}$  **do**
- 4:      $\hat{\mathbf{x}}_g \leftarrow \text{InstanceNorm}(\mathbf{x}_g)$ ; {Eq. (6)}
- 5:      $\mathbf{v}_g \leftarrow w_{\text{base}}\sigma(\hat{\mathbf{x}}_g) + \sum w_k \varphi_k(\hat{\mathbf{x}}_g)$ ; {Eq. (7), Eq. (9)}
- 6:   **end for**
- 7:   Concatenate  $\{\mathbf{v}_g\}$  and reshape to matrix form ( $B$  or  $A$ );
- 8:   **return** Matrix;
- 9: /\* Training Phase \*/
- 10: **for** epoch  $t \leftarrow 1$  to  $T$  **do**
- 11:   **for** each minibatch  $\{x, y\}$  in training data **do**
- 12:     /\* 1. Synthesize Rank Matrices via Generators \*/
- 13:      $B \leftarrow \text{GENERATOR}(Z_B, \Theta_B)$ ; {Synthesize  $B$  from Latent  $Z_B$ }
- 14:      $A \leftarrow \text{GENERATOR}(Z_A, \Theta_A)$ ; {Synthesize  $A$  from Latent  $Z_A$ }
- 15:     /\* 2. Forward pass with Adapter \*/
- 16:      $\Delta W \leftarrow BA$ ;
- 17:      $h \leftarrow W_0x + \Delta Wx$ ; {Eq. (1)}
- 18:     Compute loss  $\mathcal{L}(h, y)$ ;
- 19:     /\* 3. Backpropagate through Generators and Latents \*/
- 20:     Update  $\{Z_B, Z_A, \Theta_B, \Theta_A\}$  via gradient descent;
- 21:   **end for**
- 22: **end for**
- 23: /\* Inference Preparation (Static Merge) \*/
- 24: **Function** MERGEWEIGHTS():
- 25:    $B_{\text{final}} \leftarrow \text{GENERATOR}(Z_B, \Theta_B)$ ;
- 26:    $A_{\text{final}} \leftarrow \text{GENERATOR}(Z_A, \Theta_A)$ ;
- 27:    $\Delta W \leftarrow B_{\text{final}}A_{\text{final}}$ ; {Construct effective update}
- 28:    $W \leftarrow W_0 + \Delta W$ ; {Merge into backbone}
- 29:   **return**  $W$ ;

---

responsible for projecting back to the high-dimensional space, fixing its latent representation severely limits the flexibility of the update direction.

Notably, although freezing latents reduces the parameter count (e.g., to 0.39M), the trade-off in performance is severe. These findings confirm that the learnability of latent vectors is a fundamental component of GenLoRA, allowing the model to dynamically adjust the topological input to the RBF generators to synthesize optimal rank components.

## G. Extended Scalability Analysis and Parameter Efficiency

In our main experiments (Table 1), we configured GenLoRA with a rank of  $r = 8$  to maintain an ‘Iso-Rank’ alignment with standard baselines such as LoRA and DoRA. Additionally, we included a setting of  $r = 32$  to validate our core hypothesis: that GenLoRA enables the utilization of significantly higher ranks to unlock superior performance, all while maintaining a highly compact parameter footprint. Even at  $r = 32$ , GenLoRA requires only 2.16M parameters, which is less than half of the standard LoRA at  $r = 8$  (4.72M), demonstrating its capability to trade minimal parameters for substantial rank increases.

We did not prioritize a strict ‘Iso-Parameter’ comparison in the main results for two primary reasons. First, due to the structural differences between explicit matrix factorization and our generative approach, precise parameter alignment is geometrically constrained by integer hyperparameters such as rank and group size, making exact matching computationally infeasible without altering the model architecture. Second, and more importantly, the primary objective of this work is to demonstrate that GenLoRA can achieve superior performance by efficiently scaling up the rank with significantly fewer

Table 7. Ablation study on the learnability of latent vectors evaluated on LLaMA-3-8B (Math10K). “Frozen” indicates that the corresponding latent vectors were not updated during training.

| Method                       | #Params | Avg          |
|------------------------------|---------|--------------|
| LoRA ( $r = 8$ )             | 4.72M   | 67.87        |
| GenLoRA ( $r = 8, g = 16$ )  | 0.98M   | <b>70.17</b> |
| GenLoRA (Frozen $Z_A, Z_B$ ) | 0.39M   | 60.63        |
| GenLoRA (Frozen $Z_A$ )      | 0.59M   | 62.19        |
| GenLoRA (Frozen $Z_B$ )      | 0.79M   | 61.26        |

parameters than standard methods, rather than merely competing at equal parameter counts.

To further investigate the scalability of our approach and validate that GenLoRA can effectively leverage a larger parameter budget, we conducted an extended experiment scaling the rank to  $r = 64$ . As shown in Table 8, we present the performance trajectory across ranks  $r = 8, 32$ , and  $64$ , with the group size consistently set to  $g = 16$ .

Remarkably, even at the high-rank configuration of  $r = 64$ , GenLoRA requires only 3.74M parameters, which is still approximately 20% fewer than the standard LoRA at  $r = 8$  (4.72M). In terms of performance, GenLoRA exhibits a consistent upward trajectory as the rank increases. Although the modest accuracy improvement from 71.05% to 71.12% observed when shifting from rank 32 to 64 suggests diminishing returns, the performance remains robust and superior to the LoRA baseline. This confirms that GenLoRA successfully decouples parameter cost from rank, allowing for scalable improvements in model capacity without the prohibitive memory overhead typically associated with high-rank adaptation.

Table 8. Extended comparison on Mathematical Reasoning tasks (LLaMA-3-8B) across varying ranks and parameters.

| Method              | #Params | AddSub | MultiArith | SingleEq | SVAMP | gsm8k | AQuA  | Avg          |
|---------------------|---------|--------|------------|----------|-------|-------|-------|--------------|
| LoRA( $r = 8$ )     | 4.72M   | 82.28  | 85.83      | 89.76    | 66.40 | 56.18 | 23.23 | 67.87        |
| GenLoRA( $r = 8$ )  | 0.98M   | 88.35  | 90.67      | 93.70    | 70.80 | 53.90 | 23.62 | 70.17        |
| GenLoRA( $r = 32$ ) | 2.16M   | 87.09  | 92.71      | 94.49    | 70.80 | 56.18 | 25.59 | 71.05        |
| GenLoRA( $r = 64$ ) | 3.74M   | 89.11  | 92.00      | 92.52    | 71.80 | 56.48 | 24.80 | <b>71.12</b> |

## H. Detailed Numerical Results for Singular Value Energy

To supplement the singular value analysis introduced in Section 4.5 of the main text, we provide detailed layer-wise numerical results in Table 9. This table reports the sum of squared singular values for the learned weight updates of the self-attention query projection module  $q\text{-proj}$  across all 32 transformer layers, a metric we refer to as Energy  $\sum \sigma^2$ .

These numerical values serve as the quantitative basis for the energy spectrum comparison presented in the right panel of Figure 5. The data reveals a distinct order-of-magnitude difference between the two methods. Despite possessing a larger parameter budget, Standard LoRA exhibits relatively low energy values that typically remain below 1.5 across all rank settings, suggesting that the magnitude of its weight updates is constrained. In stark contrast, GenLoRA demonstrates significantly higher energy levels with values ranging from approximately 20 to over 400.

Crucially, the table highlights the efficiency of our approach. The rank  $r = 8$  GenLoRA using only 0.98M parameters achieves an energy value of 38.03 at Layer 0, whereas the rank  $r = 32$  Standard LoRA utilizing 18.87M parameters exhibits an energy of merely 0.28 at the same layer. This represents an increase of several orders of magnitude. This result strongly corroborates our claim that GenLoRA utilizes its effective rank more efficiently to capture significant feature variations without being hindered by parameter constraints.

## I. Experiment Details

### I.1. Dataset Details

In this section, we provide detailed descriptions of the benchmarks and datasets used to evaluate the Natural Language Generation (NLG) and Code Generation capabilities of GenLoRA.

Table 9. Layer-wise Spectrum Energy Analysis. This table details the sum of squared singular values ( $\sum \sigma^2$ ) across layers. Data is split into two panels (Layers 0-15 and 16-31). GenLoRA shows orders of magnitude higher energy than Standard LoRA.

| Method        | Config (Params)  | L0    | L1    | L2    | L3    | L4    | L5    | L6    | L7    | L8    | L9    | L10   | L11   | L12   | L13   | L14   | L15   |
|---------------|------------------|-------|-------|-------|-------|-------|-------|-------|-------|-------|-------|-------|-------|-------|-------|-------|-------|
| LoRA          | $r = 8$ (4.72M)  | 0.09  | 0.15  | 0.15  | 0.16  | 0.19  | 0.24  | 0.21  | 0.18  | 0.21  | 0.17  | 0.23  | 0.22  | 0.32  | 0.32  | 0.31  | 0.36  |
|               | $r = 16$ (9.44M) | 0.14  | 0.26  | 0.25  | 0.26  | 0.31  | 0.33  | 0.33  | 0.35  | 0.30  | 0.28  | 0.36  | 0.38  | 0.52  | 0.49  | 0.45  | 0.60  |
|               | $r = 32$ (18.9M) | 0.28  | 0.42  | 0.52  | 0.47  | 0.49  | 0.57  | 0.58  | 0.58  | 0.61  | 0.50  | 0.63  | 0.64  | 0.81  | 0.77  | 0.78  | 1.05  |
| GenLoRA(Ours) | $r = 8$ (0.98M)  | 38.0  | 33.4  | 24.4  | 36.3  | 20.1  | 27.2  | 32.8  | 24.6  | 26.6  | 30.9  | 30.8  | 28.8  | 30.7  | 40.9  | 32.7  | 46.9  |
|               | $r = 32$ (2.16M) | 198.6 | 113.5 | 93.1  | 114.7 | 90.3  | 104.9 | 105.9 | 86.3  | 103.9 | 96.6  | 104.2 | 103.0 | 119.9 | 113.0 | 100.8 | 128.1 |
|               | $r = 64$ (3.74M) | 386.8 | 232.5 | 228.4 | 230.5 | 212.5 | 227.8 | 216.5 | 230.5 | 207.7 | 199.6 | 217.4 | 205.7 | 205.7 | 229.8 | 233.8 | 246.7 |
| Method        | Config (Params)  | L16   | L17   | L18   | L19   | L20   | L21   | L22   | L23   | L24   | L25   | L26   | L27   | L28   | L29   | L30   | L31   |
| LoRA          | $r = 8$ (4.72M)  | 0.40  | 0.46  | 0.46  | 0.42  | 0.51  | 0.35  | 0.43  | 0.40  | 0.44  | 0.34  | 0.39  | 0.47  | 0.51  | 0.42  | 0.48  | 0.35  |
|               | $r = 16$ (9.44M) | 0.59  | 0.70  | 0.74  | 0.64  | 0.75  | 0.58  | 0.66  | 0.73  | 0.74  | 0.57  | 0.70  | 0.71  | 0.78  | 0.70  | 0.75  | 0.70  |
|               | $r = 32$ (18.9M) | 0.89  | 1.10  | 1.12  | 0.99  | 1.16  | 0.98  | 1.15  | 1.07  | 1.09  | 0.97  | 1.09  | 1.03  | 1.21  | 1.23  | 1.21  | 0.97  |
| GenLoRA(Ours) | $r = 8$ (0.98M)  | 37.1  | 54.7  | 53.0  | 57.5  | 57.2  | 46.4  | 49.7  | 55.6  | 36.2  | 39.5  | 54.1  | 44.1  | 66.8  | 75.8  | 55.5  | 40.7  |
|               | $r = 32$ (2.16M) | 121.0 | 161.8 | 164.7 | 143.1 | 142.5 | 139.1 | 138.5 | 152.7 | 140.1 | 138.3 | 158.7 | 163.7 | 135.0 | 226.2 | 173.4 | 131.3 |
|               | $r = 64$ (3.74M) | 255.7 | 334.8 | 294.6 | 293.5 | 264.9 | 312.2 | 286.1 | 319.9 | 287.0 | 287.7 | 332.6 | 297.0 | 320.4 | 426.9 | 326.8 | 256.5 |

**Mathematical Reasoning** We evaluate the mathematical reasoning capability of our model using the **Math10K** benchmark (Hu et al., 2023). This benchmark consists of a curated training corpus and requires the model to perform multi-step arithmetic and logical reasoning. We assess performance across the following six sub-tasks:

1. **AddSub** (Hosseini et al., 2014): A dataset of arithmetic word problems focusing on addition and subtraction operations.
2. **MultiArith** (Roy & Roth, 2016): A dataset designed to test the model’s ability to solve multi-step arithmetic problems involving various operations.
3. **SingleEq** (Koncel-Kedziorski et al., 2015): Comprises algebra word problems that map to single linear equations.
4. **SVAMP** (Patel et al., 2021): A challenge dataset created by applying variations to existing word problems to test robustness against linguistic perturbations.
5. **GSM8K** (Cobbe et al., 2021): A dataset of high-quality, linguistically diverse grade school math word problems requiring multi-step chain-of-thought reasoning.
6. **AQuA** (Ling et al., 2017): A large-scale dataset of algebra word problems with multiple-choice options, requiring complex reasoning and derivation.

**Commonsense Reasoning** We evaluate our model on the **Commonsense170K** benchmark (Hu et al., 2023), which aggregates multiple datasets for training and evaluation. The evaluation covers the following eight sub-tasks:

1. **BoolQ** (Clark et al., 2019): A binary question-answering task where the goal is to determine whether the answer to a question about a given passage is “yes” or “no.”
2. **PIQA** (Physical Interaction Question Answering) (Bisk et al., 2020): Focuses on reasoning about physical commonsense to select the most plausible solution to a given problem.
3. **SIQA** (Social IQa) (Sap et al., 2019): Tests social commonsense reasoning by asking questions about motivations, reactions, or outcomes in social contexts.
4. **HellaSwag** (Zellers et al., 2019): A task designed to test contextual commonsense reasoning by selecting the most plausible continuation of a given scenario.
5. **WinoGrande** (Sakaguchi et al., 2021): A pronoun coreference resolution task that requires reasoning over ambiguous pronouns in complex sentences.

6. **ARC-e** (AI2 Reasoning Challenge - Easy) (Clark et al., 2018): A multiple-choice question-answering task focused on elementary-level science questions.
7. **ARC-c** (AI2 Reasoning Challenge - Challenge) (Clark et al., 2018): A more difficult subset of ARC, containing questions that require advanced reasoning and knowledge retrieval.
8. **OBQA** (OpenBookQA) (Mihaylov et al., 2018): A question-answering task requiring reasoning and knowledge synthesis from a provided “open book” of science facts.

**Code Generation** We assess the code generation capability of GenLoRA by fine-tuning on the **Magicoder-Evol-Instruct-110k** dataset (Wei et al., 2023) and evaluating on the HumanEval+ benchmark.

1. **Training Data (Magicoder-Evol-Instruct-110k)**: A curated and decontaminated subset of WizardCoder (Luo et al., 2023). It comprises approximately 110k high-quality instruction-response pairs developed via the Evol-Instruct method, designed to enhance the complexity and diversity of programming tasks.
2. **Evaluation Benchmark (HumanEval+)**: An extended version of the HumanEval benchmark used to rigorously test functional correctness in code generation. We follow the standard evaluation protocol via the BigCode Evaluation Harness (Allal et al., 2022), generating 50 sampled completions per problem ( $n = 50$ ) and reporting **Pass@1**, **Pass@5**, and **Pass@10** accuracy scores.

## I.2. Baseline Details

In this section, we briefly describe the baseline methods compared in our experiments:

- **DoRA** (Liu et al., 2024a) decomposes pretrained weights into magnitude and direction components, optimizing the magnitude vector while utilizing LoRA for direction updates.
- **MELoRA** (Ren et al., 2024) introduces mini-ensemble low-rank adapters that collectively achieve high-rank expressive power.
- **HiRA** (Huang et al., 2025) utilizes the Hadamard product to enable high-rank adaptation, thereby maintaining parameter efficiency without sacrificing model capacity.
- **Aurora** (Dong et al., 2025) addresses the low-rank bottleneck by introducing nonlinear mappings within the adapter architecture to enhance expressivity.

## I.3. Implementation Details

**Details of Motivation Experiment.** To ensure fairness and generality, we conducted this analysis on standard, publicly available pretrained LoRA checkpoints. We selected the `hf1/llama-3-chinese-8b-instruct-lora` adapter (based on Meta Llama-3-8B) as our representative data source. Specifically, we extracted the `lora_A` and `lora_B` weight matrices corresponding to the Self-Attention Query Projection (`q_proj`) from the first transformer layer to serve as the ground truth for our experiments. To reconstruct these basis vectors, we formulated a regression task where the RBF generators map a shared prototype vector derived by averaging the extracted rows to the specific target basis vectors. The training objective was to minimize the element-wise Mean Squared Error (MSE) between the synthesized vectors and the ground truth. Optimization was performed using the Adam optimizer with a learning rate of  $1 \times 10^{-3}$ . The training process spanned 2,000 epochs on a single NVIDIA GPU, with no weight decay applied, to ensure rigorous convergence to the target weight patterns.

**Initialization Strategy.** To ensure stable training convergence and preserve the pre-trained model’s behavior at the onset of fine-tuning, GenLoRA replicates the “zero-initialization” property of standard LoRA (where  $\Delta W = 0$ ). Based on our implementation, we apply an asymmetric initialization strategy: (1) **For Matrix A**: The latent vector  $Z_A$  is initialized using Kaiming Uniform initialization (He et al., 2015) to introduce diverse initial variance. Correspondingly, the RBF generator weights ( $\Theta_A$ ) are initialized from a normal distribution scaled by  $1/\sqrt{d_{\text{group}}}$ . Crucially, the weights for each of the  $r$  generator functions are independently sampled from a normal distribution, ensuring that the synthesized basis vectors

are distinct and non-degenerate. (2) **For Matrix  $B$ :** Both the latent vector  $Z_B$  and the RBF generator weights ( $\Theta_B$ ) are explicitly initialized to zeros. Consequently, the synthesized matrix  $B$  starts as a zero matrix, ensuring that the total update  $\Delta W_{\text{Gen}} = BA$  is strictly zero. This guarantees that GenLoRA begins fine-tuning from an identity mapping relative to the pre-trained backbone.

**Hyperparameters and Experimental Setup** All experiments were conducted on NVIDIA RTX A6000 GPUs. The training setup utilized the AdamW optimizer (Loshchilov & Hutter, 2017) with linear learning rate decay, a LoRA dropout rate of 0.05, and no weight decay. For the code generation task, we employed a learning rate of  $2 \times 10^{-4}$ . Regarding the reasoning tasks, we set the learning rate to  $1 \times 10^{-4}$  for mathematical reasoning and  $5 \times 10^{-3}$  for commonsense reasoning. Notably, for the HiRA baseline, we adopted a unified learning rate of  $3 \times 10^{-3}$  across tasks to accommodate its distinct adaptation mechanism. Across all tasks, GenLoRA and the baseline methods were applied to the query, key, and value weights, training for one epoch with 100 warm-up steps. Our implementation builds upon the code from (Hu et al., 2023). Regarding the RBF generator configuration, we set the number of uniform centers to  $K = 15$  distributed over the fixed interval  $[-3, 3]$  to align with the instance-wise normalized inputs. Accordingly, the bandwidth  $h$  is explicitly defined by the grid spacing as  $h = \frac{6}{K-1}$ . In our comparative analysis, we primarily aligned the baseline methods to a rank of 8 to maintain a comparable parameter budget. Specifically, LoRA, DoRA, and HiRA were evaluated at rank 8. For MELORA, we adhered to the standard setting of rank 8 with four mini-ensemble groups. Regarding Aurora, we conducted tests at both rank 2 and rank 8 to specifically investigate its capability in mitigating the low-rank bottleneck through nonlinear mappings. For our proposed GenLoRA, we evaluated various configurations with differing ranks and group sizes. It is worth noting that GenLoRA consistently requires significantly fewer parameters than the rank 8 baselines; notably, some configurations involve fewer parameters than even the rank 2 Aurora setting, while achieving superior performance.